Multiple regimes of constrained chromosome motion are regulated in the interphase *Drosophila* nucleus

Julio Vazquez*, Andrew S. Belmont† and John W. Sedat*

Background: Increasing evidence indicates specific changes in the three-dimensional organization of chromosomes in the cell nucleus during the cell cycle and development. These changes may be linked to changes in both the coordinated regulation of gene transcription and the timing of chromosome replication. While there is cytological evidence for short-range diffusive motion of chromosomes during interphase, the mechanisms for large-scale chromosome remodeling inside the nucleus remain unknown.

Results: Chromosome motion was tracked in *Drosophila* spermatocyte nuclei by 3D fluorescence microscopy. The Lac repressor/*lac* operator system was used to label specific chromosomal sites in live tissues, allowing extended observation of chromatin motion in different cell cycle stages. Our results reveal a highly dynamic chromosome organization governed by two types of motion: a fast, short-range component over a 1–2 s time scale and a slower component related to long-range chromosome motion within the nucleus. The motion patterns are consistent with a random walk. In early G2, short-range motion occurs within a small, approximately 0.5 μm radius domain, while long-range motion is confined to a much larger, chromosome-sized domain. Progression through G2 as cells approach meiotic prophase is accompanied by a complete arrest of long-range chromosome motion.

Conclusions: Our analysis provides direct evidence for cell cycle-regulated changes in interphase chromatin motion. These changes are consistent with changes in local and long-range constraints on chromosome motility. We propose that dynamic interactions between chromosomes and internal nuclear structures modulate the range and rate of interphase chromatin diffusion and thereby regulate large-scale nuclear chromosome organization.

Addresses: *Department of Biochemistry and Biophysics. University of California at San Francisco. San Francisco, CA 94143. †Department of Cell and Structural Biology. University of Illinois, Urbana-Champaign. Urbana, IL 61801.

Correspondence: John W. Sedat
E-mail: sedat@msg.ucsf.edu

Received: **9 April 2001**
Revised: **29 June 2001**
Accepted: **2 July 2001**

Published: **21 August 2001**

Current Biology 2001, 11:1227–1239

0960-9822/01/$ – see front matter

Background

Studies of interphase chromosome organization have revealed a high degree of order (reviewed in [1, 2]). In many systems, including insects, plants, and vertebrates, individual chromosomes occupy distinct, nonoverlapping nuclear territories. In *Drosophila* embryos, chromosomes display a polarized arrangement, with centromeres at one pole and telomeres at the opposite pole of the nucleus [3–5]. This "Rabl" organization may represent the persistence of the anaphase configuration during interphase. In situ hybridization experiments have also revealed a close association of specific chromosomal regions with the nuclear envelope, or with internal sites inside the nucleus, and have suggested that these regions may represent anchoring sites for interphase chromosomes [4]. The combination of these different levels of organization results in a highly nonrandom radial and axial intranuclear positioning of chromosomal loci in the *Drosophila* embryo [4].

In contrast with this highly ordered, deterministic view of nuclear organization, recent work suggests a more plastic organization of chromosomes during interphase. In *Drosophila*, the insertion of a pericentric heterochromatin block at the *brown* locus is sufficient to relocate the distal end of chromosome 2R inside the nucleus [5, 6]. Loss of the Rabl configuration is observed at distinct stages of development and cell cycle progression [5, 7], while major changes in the 3D organization of chromosomes during development are associated with homologous pairing [8, 9]. Finally, relocalization of chromosomal sequences bound by the insulator protein suppressor of Hairy-wing correlates with gene transcription [10].

In yeast and mammalian nuclei, the spatial positioning of chromosomal domains may be critical for the correct regulation of chromosome replication [11, 12]. In mammalian nuclei, such positioning is established early during G1. However, several specific chromosome regions have been shown to reproducibly reposition within the nucleus either at distinct stages within the cell cycle or as a func-

tion of gene regulation ([13–18]; reviewed in [2, 19, 20]). Unknown at this time are the mechanisms which direct specific chromosome regions to defined regions within the nucleus and how chromosome regions move between different locations.

Direct evidence for chromatin motion has been obtained from cytological studies of live cells. Using GFP-tagged chromosomes and single-particle tracking in *S. cerevisiae*, Marshall et al [21] showed that a well-defined interphase chromatin region near the centromere of chromosome III is subject to Brownian motion, confined to a small territory ($r \leq 0.25$ μm) within the nucleus. A similar type of constrained, but apparently Brownian, motion was observed for the 359 bp heterochromatic repeat on *Drosophila* chromosomes labeled with fluorescent topoisomerase II [21]. Consistent with these results, several studies in mammalian cells did not reveal substantial chromatin motion during interphase [22–24]. While these results provide evidence for some degree of short-range Brownian motion, they leave many open questions. For instance, it is unclear whether the levels and range of diffusive motion observed are sufficient to account for the rapid and dramatic remodeling of chromosomes observed in a variety of systems or whether additional mechanisms might be required for the spatial remodeling of chromosomes.

Here, we report real-time analysis of chromosome motion in a developing tissue. Combining the Lac repressor/*lac* operator system with single-particle tracking analysis, we were able to follow the motion of tagged chromosomal sites in the live, developing spermatocyte nucleus in *Drosophila*. Our results reveal a high degree of local and long-range motion compatible with rapid remodeling of nuclear architecture. We find different temporal regimes of motion, consistent with different levels of organization of the chromatin fiber. We also observe dramatic changes in the pattern and rate of motion as cells progress through interphase. Finally, our results show the confinement of chromosomes to specific nuclear territories even in the presence of a high degree of chromatin motion. The results support a model for the dynamic organization of interphase chromatin based on diffusive motion modulated by local interactions.

Results

Tracking interphase chromatin motion in spermatocyte nuclei

The Lac repressor/*lac* operator system has been previously used for the visualization of 1–10 kb arrays of *lac* operator sites in live yeast [25], bacteria [26, 27], and mammalian cells [28]. To label discrete chromosomal sites in live *Drosophila* nuclei, we used P element-mediated transformation to generate transgenic strains that expressed a nuclear GFP-Lac repressor fusion protein (GFP-LacI) in different tissues (Figure 1a). The target for the GFP-LacI protein was provided by a 10.1 kb array of 256 *lac* operator (*lac* O) sequences integrated at different euchromatic sites (Figure 1b).

Figure 1

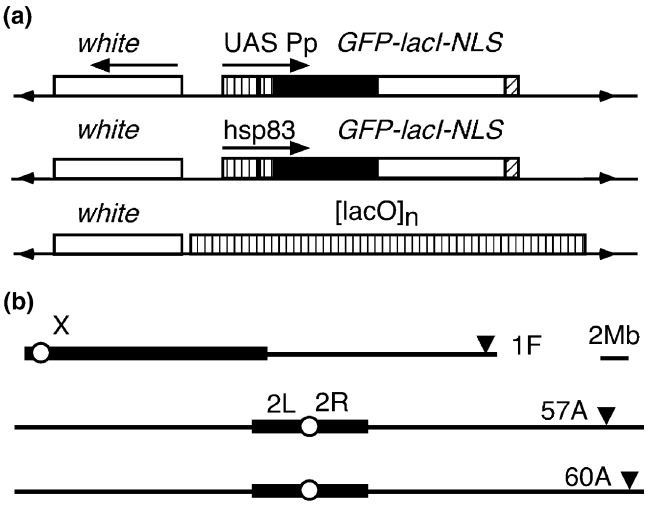

Experimental system. **(a)** Structure of the P element vectors used for this study. A GFP-Lac repressor fusion (GFP-LacI) was expressed either from a GAL4-UAS-P transposase promoter or from a constitutive *Drosophila hsp83* promoter. The SV40 NLS was used for targeting the protein to nuclei. An array containing 256 copies (approximately 10 kb) of the *lac* operator (*lac* O) sequence was used as a target for GFP-LacI. **(b)** Summary of the *lac* O insertion lines. Euchromatic P[*lac* O] inserts at cytological map positions 1F (X chromosome) and 57A and 60A (second chromosome) were used in this study. Heterochromatic regions are represented as filled boxes.

GFP-LacI was predominantly nuclear in all expressed *Drosophila* tissues and was uniformly distributed within the nucleus. The number of nuclear GFP dots correlated with the number of chromosomal *lac* O inserts (J.V. and J.W.S., unpublished data). Occasionally, some of the *lac* O inserts appeared as two distinct, closely located dots. Such duplicated sites may represent unpaired homologs or chromosomes in the process of replication.

To follow chromosome motion during development, we chose to focus on the *Drosophila* male germline. This system has been well characterized at the cytological level and is well suited for developmental and genetic studies [29]. Individual cysts develop autonomously and can be cultured in vitro under conditions that allow the continuation of their developmental program for extended periods of time [30]. It is therefore possible to follow the entire germline developmental pathway under the microscope. Gonads from third-instar larvae were dissected, and 16-cell cysts were cultured in a sealed microscope chamber [30]. Spermatocytes at different stages of development were identified by morphological criteria ([31]; Figure 2).

Figure 2

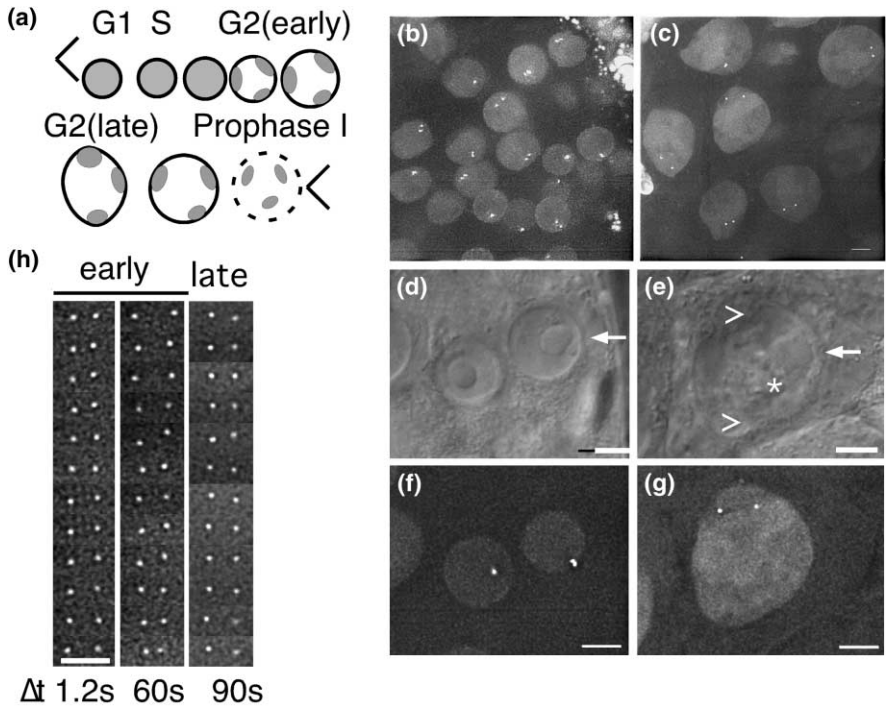

Visualization of tagged chromosomes in spermatocyte nuclei. **(a)** Summary of spermatocyte development. The diagram shows spermatocyte nuclei at different stages of premeiotic interphase, starting with the last gonial mitotic division and leading to the first meiotic division. Shaded areas represent chromatin. "Early" corresponds to nuclei in mid-G2, soon after the separation of chromatin into three clusters (nuclear diameter = approximately 10 μm). "Late" corresponds to nuclei in late G2, before the onset of meiotic prophase (irregular nuclear shape; diameter = 14–17 μm). These two stages correspond approximately to stages S3 and S5 as described [31]. **(b–g)** Visualization of tagged chromosomes in spermatocyte nuclei. The top row shows a field of (b) early and (c) late nuclei heterozygous for a single *lac* O insert at position 60A on chromosome 2. Nuclei are visible due to the presence of nuclear GFP-LacI. (d–g) higher-magnification view of (d,f) early and (e,g) late spermatocyte nuclei. (d) and (e) are DIC images. Note the well-defined nucleoli (arrow). The autosomal bivalents appear as distinct masses in late nuclei (arrowheads). Also visible are the Y chromosome loops (*) in close proximity to the nucleolus. (f) and (g) show fluorescence images of the same nuclei revealing the *lac* O arrays labeled with GFP-LacI. Most nuclei show two dots because of the separation of sister chromatids. In a few early nuclei, sisters may be paired, resulting in a single dot. **(h)** Time lapse movies of chromatin motion in early and late spermatocyte nuclei. Three movies are shown (reading from top to bottom). The two dots correspond to the two sister chromatids from a single *lac* O insert at site 1F on the X chromosome. The time intervals between frames are indicated. Scale bars represent 5 μm.

We restricted our analysis to two readily identifiable stages of premeiotic interphase. The first stage, "early," is characterized by cells with an asymmetrically located round nucleus with a diameter of about 10–11 μm and a well-defined, round nucleolus. This stage corresponds to spermatocytes in mid G2, in which replicated chromosomes have separated into three clusters, representing the three major chromosome pairs. The second stage, "late," consists of mature spermatocytes in late G2, approximately 6–12 hr before the onset of meiosis. These cells are characterized by a large, irregular nucleus of approximately 14–17 μm in diameter and an irregular nucleolus. These two stages correspond approximately to stages S3 and S5, described in [31].

Dissected testes were cultured for up to 14 hr. During this time, cysts retained a spherical, 3D organization, and spermatocytes continued their normal developmental program, as indicated by characteristic changes in size and morphology. In particular, mature spermatocytes successfully completed both meiotic divisions in vitro after several hours of imaging (data not shown). No differences in nuclear morphology or chromosome organization were observed between spermatocytes cultured for up to 10–12 hr and freshly dissected spermatocytes at similar stages of development. After longer periods of time, morphological differences became apparent, and the development of a substantial proportion of cells was delayed or arrested [30].

GFP-LacI could be readily detected as a sharp, bright dot when bound to its target *lac* O array in live spermatocyte nuclei (Figure 2b–g). Generally, the width of the intensity peak of the fluorescent dots, at half-maximum intensity, was approximately 3 pixels (approximately 0.33 μm), similar to that of 0.1 μm fluorescent beads and consistent with a subresolution point source. These results suggest a substantial degree of compaction for the 10 kb *lac* O array, possibly at the level of a 30 nm fiber. In young spermatocytes (including those in G1, S, and the beginning of G2), nuclei heterozygous or homozygous for a single *lac* O insert displayed a single GFP dot, as expected from paired chromosomes. Surprisingly, in middle to late G2, heterozygous nuclei displayed two GFP dots, while homozygous lines displayed four dots; these findings are consistent with the unpairing of homologous chromosomes and the separation of sister chromatids. This separation was observed at all sites tested (a total of nine euchromatic insertions on the X, 2nd, and 3rd

chromosomes; our unpublished data). Furthermore, the separation was not a result of culture conditions since it was observed in freshly dissected, whole testes and appeared to be stage specific. Since such gross differences in chromosome structure are expected to affect their diffusion characteristics, we restricted our analysis to similarly organized, unpaired chromosomes in middle and late G2.

To track the motion of GFP-tagged loci, we recorded time-lapse movies of nuclei heterozygous for a single *lac* O insert (Figure 2h). Chromosome motion was quantitated by a plot of the distance between two moving loci as a function of time. Since the center of mass of individual dots can be determined with greater accuracy than the center of mass of an entire nucleus, this approach offered high spatial resolution while minimizing the effects of nuclear translation or rotation. The error in these distance measurements was estimated to be less than 50 nm [21]. Fast imaging rates were obtained by the selection of nuclei with both dots on a single focal plane; this method allowed the collection of time-lapse 2D sections at 0.5–1 frames/s. For analysis of motion over longer time periods, 3D images of entire nuclei were collected at a lower sampling frequency.

Figure 3

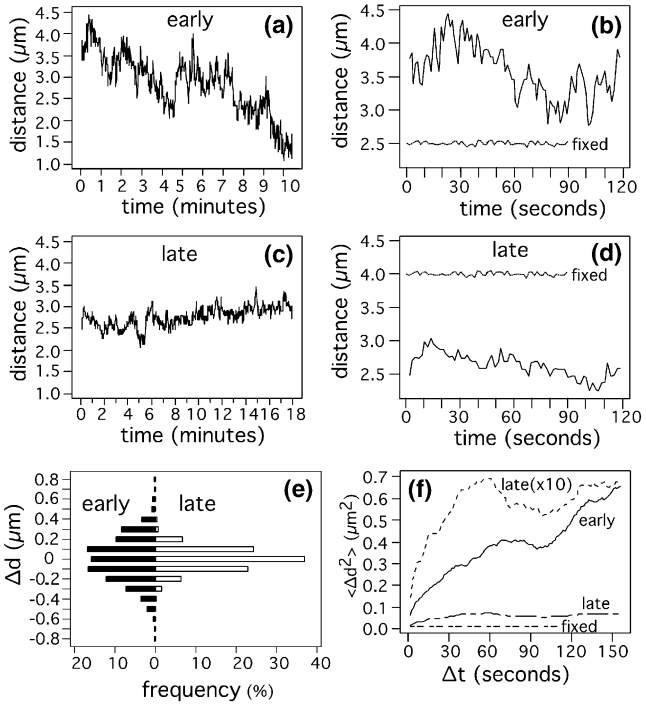

Chromatin motion in spermatocyte nuclei. The single X chromosome was tagged at site 1F. Time plots of the distance between the two sister loci in **(a,b)** one early and **(c,d)** one late nucleus are shown in two different time scales. The early nucleus shown here was imaged for 11 min at a rate of one 2D frame (single optical section) every 1.2 s. The late nucleus was imaged for 17 min at a rate of 1 frame every 1.7 s. **(e)** shows the distribution of Δd values for one time interval (Δt = 1.2 s for early nuclei and 1.7 s for late nuclei, respectively). The standard deviations of the distributions are 0.24 μm (early) and 0.12 μm (late). The standard deviation in fixed nuclei was 0.07 μm (not shown). **(f)** shows a plot of the mean square change in distance ($<\Delta d^2>$) for early (continuous line) and late nuclei (broken line; dotted line = $<\Delta d^2> \times 10$). As a control, a time plot of the distance between two GFP dots in a representative fixed nucleus has been indicated in (b) and (d) (the absolute position on the *y* axis is arbitrary). The corresponding $<\Delta d^2>$ values were calculated and plotted in (f) (approximately 4×10^{-3} μm² at all time intervals). At least 20 nuclei were imaged for each stage. The general features of the random walks shown here are representative for the different types of nuclei.

Brownian motion of chromatin

Examples of chromatin motion are shown in Figure 3a–d. Substantial motion was detected in early and late nuclei, for time intervals as small as 1–2 s. Figure 3e shows a histogram of the changes in distance (Δd) at small time intervals for two representative nuclei. In early nuclei, the Δd values followed a normal distribution (mean ≈ 0, and standard deviation ≈ 0.24 μm), with maximum values up to ± 0.8 μm. On average, the direction of individual runs changed approximately every two seconds (as determined by the change in sign for Δd), and only a small fraction of the runs (approximately 6%) did not change direction for four time points or longer. These results, together with the analysis of time-lapse movies and time plots, suggest that the motion of chromatin in early spermatocyte nuclei is a random walk since there was no evidence for substantial directed motion. The estimated step size ∂x along each axis for individual dots in early nuclei was approximately 0.17 μm in a 1.2 s interval and corresponded to a 3D step size of approximately 0.3 μm. Over longer time periods, substantial displacements were observed, with Δd values up to 1.5 μm in 1 min and up to 3 μm over 10 min (Figure 3a–b).

In unobstructed diffusion, the mean square displacement (MSD) is proportional to time. One can obtain the MSD by averaging over a large ensemble of molecules (as in FRAP) or over a large number of time points (as in single-particle tracking). For a single object performing a random walk, statistical fluctuations in the MSD values are expected. The plot of MSD as a function of time, however, should approximate a straight line, provided that the number of averaged time points is fairly large (a condition that was met in our experiments, with $N \geq 500$ time points per nucleus). In practice, we found that the approximation was reasonably good for Δt values up to 25%–30% of the entire collection period. For longer time intervals, the statistical fluctuations increase, and this increase leads to significant departures from linearity for individual random walks [32, 33]. In our experiments, the MSD could not be directly determined. Instead, a different value, the mean square change in distance between two points ($<\Delta d^2>$, proportional to MSD) was calculated (Materials and methods). A plot of $<\Delta d^2>$, in early nuclei, showed

a fairly linear increase as a function of time; such an increase is characteristic of diffusive motion (Figure 3f). We determined the mean slope of the curve by fitting a least-squares regression line for all data points falling approximately in the linear range ($\Delta t \geq 30$ s). The slope of this line provided a measure of the average diffusion coefficient for individual *lac* O sites: $D = <\Delta d^2>/4\Delta t = 8.3x10^{-4}$ $\mu m^2/s$.

To determine whether this estimate of D was representative, we calculated and averaged the $<\Delta d^2>$ curves for 11 different nuclei that were imaged for 3–10 min. The individual curves showed substantial variability, similar to the variability observed between different time segments for a given nucleus (data not shown). Such variability could be attributed to the random-walk nature of the motion [32, 33]. The average of all nuclei provided a value of approximately 1.0×10^{-3} $\mu m^2/s$ for the apparent diffusion coefficient of single sites in early nuclei. This value is comparable to the value of 2.0×10^{-3} $\mu m^2/s$ obtained for the diffusion of chromatin in early *Drosophila* embryonic nuclei, and it is about one order of magnitude greater than the diffusion coefficient of chromatin in yeast [21]. At this rate, a given locus is expected to diffuse on average 4.6 μm in 1 hr.

Different rates of motion in early and late nuclei

To determine whether rates of chromatin motion can change during the cell cycle, we performed a similar analysis on mature spermatocytes in late G2 (late nuclei; Figures 2h and 3c–d). A representative plot of the distance between two GFP dots in late nuclei is shown in Figure 3c. In this example, the distance between the two loci remained relatively constant over a 17 min period, with a maximum change in distance, Δd, of 1.4 μm. The Δd values for $\Delta t = 1.7$ s followed a normal distribution, with zero mean and a standard deviation of 0.12 μm (Figure 3e). We calculated an average step size, ∂x, of 0.08 μm for individual sites (for $\Delta t = 1.7$ s); this was approximately half the value found in early nuclei. The 3D step size was approximately 0.15 μm. Displacements were relatively small but were still significantly different from those observed in fixed nuclei (estimated $\partial x \leq 0.04$ μm) that served as a control. More importantly, $<\Delta d^2>$ in fixed nuclei did not increase with longer time intervals, as expected if the apparent motion in fixed nuclei is mostly due to measurement errors.

The diffusion coefficient for chromatin in late nuclei was determined from the $<\Delta d^2>$ values. As shown in Figure 3f, the plot had a fairly steep slope at small time intervals ($\Delta t \leq 30$ s) and reached a peak value of $<\Delta d^2> = 0.06$ μm^2 at $\Delta t = 1$ min (which corresponds to an average change in distance of about 0.25 μm). There was little increase in $<\Delta d^2>$ for longer time periods, consistent with severe constraint on chromatin motion. A least-squares fitted line on the values for $\Delta t \geq 30$ s indicated an average diffusion coefficient for individual *lac* O loci of approximately 5×10^{-5} $\mu m^2/s$, a value approximately 30 times smaller than that observed in early nuclei. The value of D, determined under similar conditions, for a fixed nucleus was $\leq 2 \times 10^{-6}$ $\mu m^2/s$. The differences in chromosome motion in early and late nuclei were confirmed by statistical analysis of the distributions of $<\Delta d>$ values (see the Supplementary material available with this article on the internet). This analysis also revealed an unexpected anomaly in the diffusion of chromatin in early and late nuclei at $\Delta t = 5$–10 s (see below).

Anomalous diffusion of chromatin

Analysis of the $<\Delta d^2>$ plots revealed significantly steeper slopes at very short time intervals ($\Delta t \leq 4$ s; Figure 3f). This feature was observed in all nuclei examined (>80) and could not be explained by random statistical fluctuations. On the other hand, the $<\Delta d^2>$ plot was fairly linear for simulated random walks and also for freely diffusing latex beads imaged and analyzed under similar conditions (data not shown). This finding ruled out instrumentation and/or data analysis as the source of the anomaly. For freely diffusing objects, the diffusion coefficient is independent of time, and a plot of MSD/Δt as a function of Δt should yield a horizontal line whose intercept equals 4D. Departures from linearity of the MSD/Δt plot may be indicative of anomalies in the diffusion rates and therefore reveal unsuspected components for the observed motion [34]. To further characterize this anomalous diffusion, we plotted ($<\Delta d^2>/\Delta t$) as a function of Δt (Figure 4a,b).

We observed a strong deviation from linearity of the ($<\Delta d^2>/\Delta t$) plot at small time intervals. In both early and late nuclei, the apparent diffusion coefficient was greater when it was determined over the smallest time interval, and it rapidly declined over the first 10–20 s. At longer time intervals, the plot became linear, which indicated a fairly constant diffusion coefficient. The shape of the curve suggests that the actual diffusion coefficient, at small time intervals, decreases approximately as the inverse of time. Such a behavior is consistent with the severely constrained diffusion of a particle within a small territory, where the boundary of confinement is reached in a time scale comparable to our sampling interval $\Delta t_{min} = 1.2$ s. A similar curve can be obtained for a simulated, strongly constrained random walk and is observed for fixed samples, in which most of the motion is due to noise and occurs at very small time intervals (Figure 4c). Under these conditions, the actual diffusion coefficient of the particle can not be accurately determined, and the value of $<\Delta d^2>$ at Δt_{min} is determined by the radius of confinement.

In fixed nuclei, curves for $<\Delta d^2(t)>/\Delta t$ and $<\Delta d^2(t_{min})>/\Delta t$ overlap, which indicates that all the motion occurs at

Figure 4

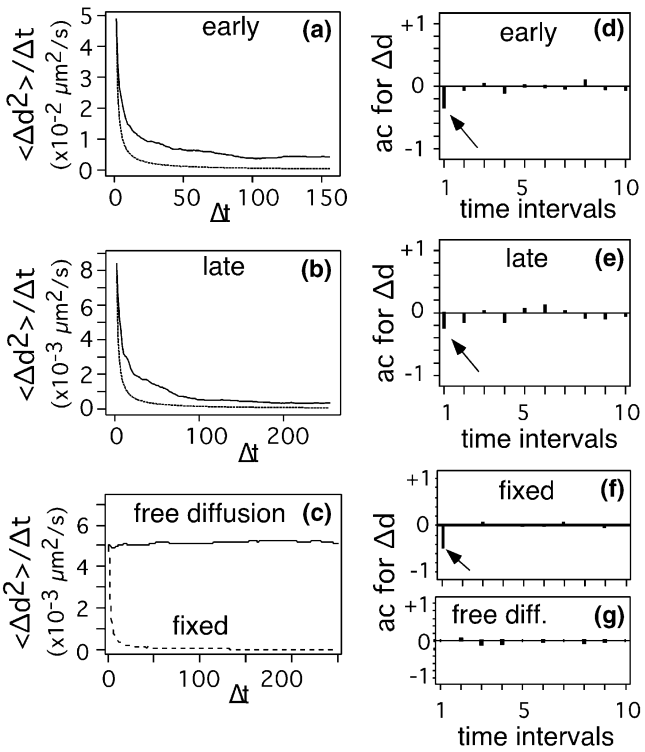

Anomalous chromosome motion. **(a, b)** Plot of $<\Delta d(t)^2>/\Delta t$ (continuous line) as a function of Δt for (a) early and (b) late nuclei. The dotted (lower) line plots $<\Delta d(\Delta t = 1)^2>/\Delta t$ as a function of Δt and provides a measure of the apparent effect of short-range diffusion on the estimate of long-range diffusion. For both types of nuclei, diffusion is approximately normal for Δt values ≥50–100 s. Note the shoulder at Δt = 20–80 s in late nuclei. **(c)** Plot of $<\Delta d^2>/\Delta t$ for free diffusion (either from simulated random walks or from actual random walks from diffusing latex beads; see Materials and methods) and for fixed nuclei (severely constrained diffusion). **(d–g)** Autocorrelation analysis. The correlation between the displacement values (Δd) for time points separated by an increasing number of time intervals is shown for (d) early nuclei, (e) late nuclei, (f) severely constrained diffusion (fixed nuclei), and (g) free diffusion (either freely diffusing latex beads or computer-simulated random walks). A significant negative value at one time interval is observed in (d) early, (e) late, and (f) fixed nuclei. (g) No correlation was present in simulated random walks or in actual random walks from diffusing beads.

time intervals $\leq \Delta t_{min}$ and that there is no further increase in displacement at longer time intervals (Figure 4b). In live nuclei, on the other hand, there is a small but significant difference between the two plots at long time intervals (Figure 4a). These results indicate that diffusion of chromatin has two components: a short-range, quasi-stationary component responsible for the relatively high diffusion coefficient at small time intervals and a long-range component that becomes apparent as Δt increases and the effects of the stationary component become negligible. The value of $<\Delta d^2>$ at Δt_{min} provides a minimum estimate of the actual short-range diffusion coefficient of chromatin (D_1), while the horizontal part of the plot represents the long-range diffusion coefficient (D_2). The values of D_1 and D_2 were estimated from a large sample of nuclei and are given in Table 1. The values for D_2 are comparable to the average values previously determined from the slope of the MSD curve. The values for the short-range diffusion coefficient D_1, on the other hand, are about 13 and 36 times higher than the long-range diffusion coefficients in early and late nuclei, respectively. These results indicate a fast, severely constrained chromatin diffusion at small time intervals in both types of nuclei. The two regimes of chromatin diffusion at short and long time intervals were also evident from the statistical analysis of the distribution of $<\Delta d>$ values (Supplementary material).

To further characterize the diffusive motion of chromatin and to search for motion patterns that might be relevant to the underlying chromosome structure, we determined the autocorrelation function (acf) for the Δd values ([35]; Figure 4d–g). The acf evaluates the serial dependence of a time series by calculating the correlation between sets of data points separated by an increasing number of time intervals. The analysis revealed a small but significant negative value at 1 Δt (Figure 4d–e). This negative value is consistent with a conserved motion pattern that occurs in a time scale of 1–2 s and probably reflects the short-scale component described above. Consistent with this idea, a similar negative value was observed in fixed nuclei (severe constraint) but was not observed in simulated random walks or in actual random walks generated by freely diffusing latex beads (free diffusion; Figure 4f–g and data not shown). This result indicates a higher probability of the *lac* O sites "bouncing back" (i.e., the Δd values do not change at random, but rather they show an increased probability of changing sign between successive time points). Such behavior is consistent with a constraint on chromatin motion that takes place at the smallest time interval ($\Delta t \leq 2$ s).

Chromatin motion in early nuclei is confined to a chromosome territory-sized region

The results presented above indicate a high degree of chromatin motion in early spermatocyte nuclei, with a long-range diffusion coefficient of about 1×10^{-3} $\mu m^2/s$ for individual *lac* O sites. At this rate, a given chromatin region is expected to travel 4.6 μm in one hour and, on average, will explore the entire nucleus (approximately 11–12 μm diameter) in approximately 6–7 hr. Therefore, two freely diffusing loci will disperse randomly inside the entire nucleus in a few hours. To determine whether chromatin is able to diffuse freely across the entire nucleus over longer time intervals, we imaged whole nuclei in 3D at intervals of 15 min for several hours. Time-lapse movies indicated that chromatin did not diffuse across the nucleus at the rates expected but rather remained confined to a small region within the nucleus. Typical results are shown

Table 1

Summary of the motion patterns.

Short range	Early	Late	Fixed
D_1	1.3×10^{-2} μm²/s	3.4×10^{-3} μm²/s	8.5×10^{-4} μm²/s
Δr_{rms} (1 s)	0.30 μm	0.15 μm	0.07 μm
N/n	37/>3000	46/>3000	3/180
Long range	**Early**	**Late**	**Fixed**
D_2	1.0×10^{-3} μm²/s	9.4×10^{-5} μm²/s	$<5 \times 10^{-6}$ μm²/s
Δr_{rms} (1 min)	0.6 μm	0.2 μm	NA
Δr_{rms} (1 hr)	4.6 μm	1.4 μm	NA
r_c	~3.0 μm	≤0.3 μm	≤0.08 μm
Δt_c	30 min	≤10 s	≤2 s
N/n	22/172	31/117	3/120

The short-range (D_1) and long-range (D_2) diffusion coefficients were calculated for early, late, and fixed spermatocytes. The transition between short-range and long-range motion occurred between $\Delta t = 2$ and $\Delta t = 10$ s. The values of D were calculated for $\Delta t = 1.2–1.7$ s (D_1), $\Delta t = 10$ min (D_2 early), or $\Delta t = 30$ min (D_2 late). The expected displacements (Δr_{rms}) for various time intervals are given. Abbreviations are as follows: r_c, estimated radius of confinement; Δt_c, estimated time required to reach the radius of confinement; N/n, number of nuclei/time points used; NA, not applicable.

in Figure 5a–b. In these nuclei, homozygous for a single insert on chromosome 2, we recorded the motion of four loci to provide a better visualization of chromatin spreading. In early nuclei (Figure 5a), the movie reveals substantial spatial reorganization of the four *lac* O sites between consecutive 3D images, and this reorganization is consistent with the previously determined diffusion coefficient of 1×10^{-3} μm²/s. On the other hand, the spreading of the sites was limited, and no further increase in interlocus distance was observed for periods longer than 30–60 min. These findings indicate a confinement of the four *lac* O sites to a small sub-volume of about 3 μm radius within the spermatocyte nucleus. The confinement is supported by a statistical analysis of the interlocus distances. As shown in the histogram (Figure 5c), the distances between sister loci in early nuclei range from 0 to 7 μm, with a mean value of approximately 2.6 μm (excluding nuclei with paired dots). The distribution of distances does not significantly change after ≥10 hr of further development, with a mean interlocus distance of 3.3 μm in late nuclei (Figure 5d). Since we imaged sister or homologous loci, a possible explanation for the constraint on the interlocus spreading could involve the pairing of homologous chromosomes or sister chromatid cohesion. The evidence sug-

Figure 5

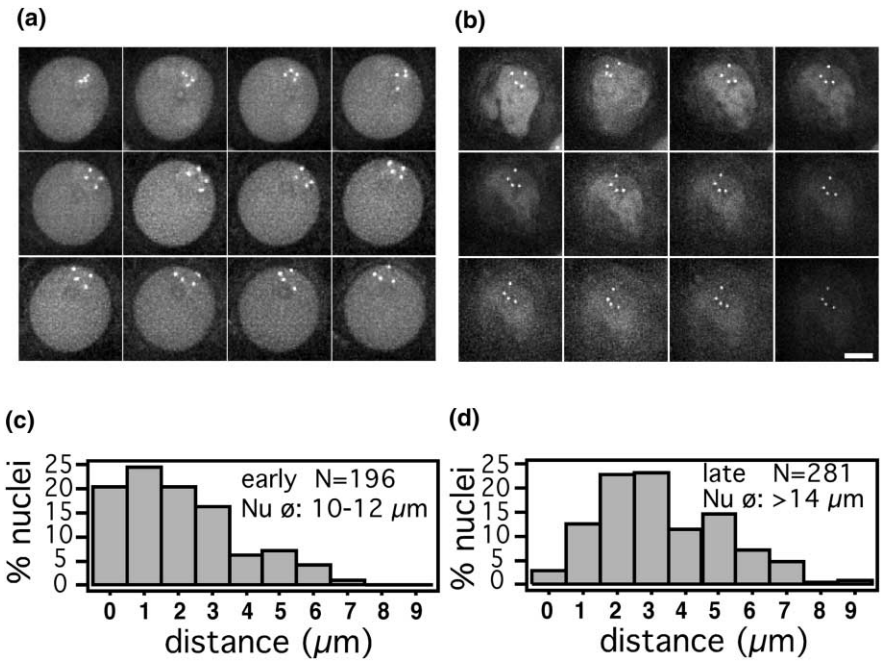

Long-range chromosome motion. **(a,b)** Time lapse movies of chromosome motion in (a) early and (b) late nuclei. Flies were homozygous for a *lac* O insert at locus 60A (2nd chromosome). 3D data sets were collected at 15 min intervals. Each image is a spatial projection of several z-sections. The scale bar represents 5 μm. **(c,d)** Distribution of interlocus distances between two sister loci in flies heterozygous for a *lac* O insert at position 60A in early nuclei (10–12 μm nuclear diameter) and late nuclei (≥14 μm nuclear diameter). The separation of sister chromatids occurs at a nuclear diameter of approximately 10 μm.

gests, however, that at this stage the association of homologs (and sister chromatids) is limited to the centromeric region (our unpublished data). We estimate that the length of the chromatin fiber, from the centromere to our tagged sites, probably exceeds 100 μm and therefore cannot account for the observed constraint, which can best be explained by local attachments on individual chromatids. Consistent with this idea, the position of individual chromosomes within the nucleus appears to be relatively fixed in spite of a high degree of motility of individual sites.

Lack of long-range chromatin motion in late spermatocytes

The time-course experiments for time intervals up to 17 min did not allow us to determine with certainty whether chromatin was subject to actual long-range motion in late spermatocyte nuclei. The distribution of the absolute displacement values between pairs of loci as a function of time, together with the analysis of the $<\Delta d^2>$ plots, suggested a moderate degree of motion at small time scales (1–60 s) but an absence of motion over time scales longer than 1 min. The diffusion coefficient of chromatin in late nuclei is very small, however, and it is possible that a long-range component could have been missed in the short time intervals used. We therefore followed the motion of *lac* O sites in 3D for extended periods of time. Time-lapse data sets taken at 15 min intervals showed little change in the distance between GFP dots, or their relative positions, for periods up to 2–3 hr (Figure 5b). This contrasted with the behavior of loci in early nuclei, which showed constant spatial reorganization.

Lack of significant long-range motion was even more apparent when nuclei were imaged at 30 min intervals for periods of several hours (see Supplementary material). Relatively invariant positions were maintained for up to 8 hr despite the dramatic changes in nuclear shape that took place as spermatocytes progressed toward meiotic prophase. All together, these results indicate a lack of long-range chromatin motion in late nuclei over periods of time greater than 1–2 min, and show confinement of individual chromosomal loci within a small radius of ≤ 0.5 μm during late G2. Consistent with the strong local constraint on chromatin motion, the results also show that whole chromosomes retain relatively invariant positions within the nucleus for extended periods of time (data not shown). Occasionally, movements of greater amplitude could be observed. A careful analysis of the time-lapse movies suggested that such movements are largely the result of large-scale nuclear deformations and are not linked to chromatin diffusion. These movements, however, do contribute to the apparent displacement of the GFP dots. As a consequence, we expect the actual long-range diffusion coefficient to be significantly smaller than the experimentally determined value of approximately 1×10^{-4} μm²/s in late G2.

Figure 6

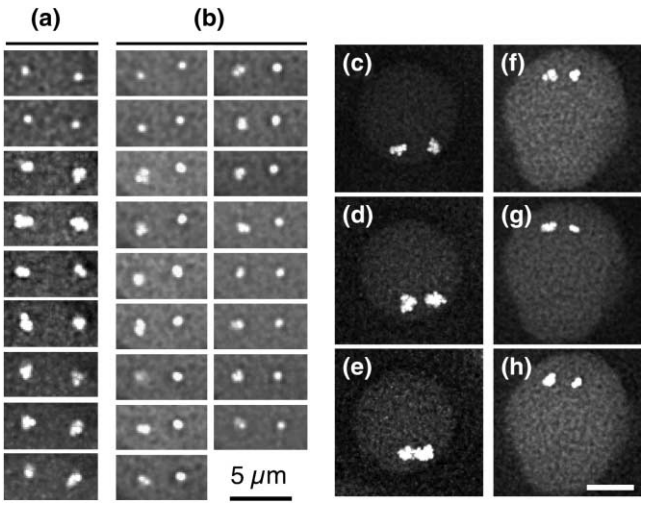

Visual evidence for short-range and long-range motion. To provide a visual representation of the spatial domain explored by individual chromosomal loci, we collected consecutive 2D images for various time intervals and projected them onto a single image frame. **(a,b)** Projections show the motion of chromatin during a 12 s period in (a) early and (b) late nuclei. The first two panels of each set are single 2D sections (movies read from top to bottom). **(c–h)** Long-range motion in (c–e) early and (f–h) late nuclei. Each panel represents a temporal projection of time lapse 2D images collected for (c) 1 or (d–h) 3 min. Consecutive panels are separated by (c–e) 5 min or (f–h) 7 min intervals. Flies are hemizygous for a single insert at position 1F (X). Two chromatids are visible.

Visual evidence for the confinement of chromatin

To obtain direct visual evidence for the different levels of motion, we examined projections of multiple frames representing consecutive time points. The short-range motion is best illustrated by an examination of projections of consecutive time points covering a 10 s period (Figure 6a–b). In early nuclei, individual GFP dots explored very similar regions of space, with an average radius of approximately 0.5–0.7 μm in 10 s intervals. This value probably overestimated chromatin motion due to the added effects of random nuclear motion but was nevertheless in good agreement with the experimentally determined displacement values between loci; these values are relatively independent of nuclear motion. For instance, the average expected displacement in early nuclei is about 0.3 μm in 1 s (Table 1). Over longer periods of time, the nuclear domain explored by individual *lac* O sites in early nuclei expanded until it covered a substantial fraction of the entire chromosomal territory in less than 15 min (Figure 6c–e). On the other hand, late nuclei showed different motion patterns for individual dots in a short time scale. The patterns ranged from loci that were apparently immo-

bile to loci that moved within a radius comparable to that observed in early nuclei (Figure 6b). Within a given nucleus, the different patterns of motion persisted over extended periods of time, and this observation suggests that they were not due to transient local random fluctuations in chromatin motility but rather to stable physical constraints. This would be consistent with the tethering of the chromatin fiber at variable distances from the labeled loci. Over longer time intervals, the domain explored by individual sites in late nuclei did not expand significantly (Figure 6f–h), and this result is in agreement with the low long-range diffusion coefficient determined for these nuclei.

Discussion

Our analysis of the motion of interphase chromosomes in *Drosophila* spermatocyte nuclei indicates that chromatin is subject to Brownian (diffusive) motion, in agreement with previous reports [21]. The motion patterns, however, reveal several unexpected features. First, we find that chromatin can move over much larger distances than previously reported, up to approximately 4–5 μm/hr. Second, there are clear and reproducible differences in the apparent diffusion coefficient of chromatin when it is measured over different time scales. These differences suggest at least two different regimes for short- and long-range motion and are likely to be due to the underlying chromosome structure. The third novel feature is a striking change in the motion patterns as cells progress through G2, suggesting a possible regulatory mechanism. Finally, our results suggest the tethering of the chromatin fiber and support a higher-order domain model for chromosome organization.

Structural implications

We found evidence for two components of chromatin motion in early G2 spermatocyte nuclei. The first component, at short time intervals, is characterized by an average step size for individual loci of approximately 0.3 μm (range: approximately 0–0.7 μm) for $\Delta t = 1.2$ s. This component results in an apparent short-range diffusion coefficient $D_1 \approx 1.3 \times 10^{-2}$ μm²/s. For longer time intervals, the MSD does not increase linearly with time, as would be expected for freely diffusing chromatin. For instance, at $\Delta t = 2.4$ s, the apparent diffusion coefficient $D = 0.9 \times 10^{-2}$ μm²/s, about 30% smaller than D_1. We interpret this pattern as indicating that chromatin has a severely constrained Brownian motion, which is characterized by a diffusion coefficient $\geq 1.3 \times 10^{-2}$ μm²/s and which occurrs in a very small territory of average radius $r_S \leq 0.3$ μm. The rapid decrease in the apparent diffusion coefficient as Δt increases suggests that the confinement boundary is reached within a time scale comparable to our sampling time. The origin of this short-range component is unclear. Such a pattern could result from the motion of a relatively small segment of chromatin tethered, perhaps transiently, to an internal nuclear site. Alternatively, this motion pattern could reflect the motion of the chromosome fiber within a crowded environment [34]. In the latter case, the radius of confinement of approximately 0.3 μm might correspond to the average distance between chromatin fibers inside the spermatocyte nucleus.

At long time intervals ($\Delta t \geq 30$ s), the contribution of the fast component becomes comparatively small, and chromatin appears to diffuse with an apparent long-range coefficient $D_2 \approx 1 \times 10^{-3}$ μm²/s that is independent of time. This diffusion coefficient is 13 times smaller than the fast component and is responsible for the slow, long-range random-walk motion of interphase chromatin within the nucleus. The diffusion coefficient in early spermatocyte nuclei is comparable to the diffusion coefficient determined in the early *Drosophila* embryo [21]. It must be noted that in these earlier studies, the lower sampling rate (one 3D data set every 10 s, approximately) would have failed to reveal the presence of a similar short-range component. The analysis of the $<\Delta d^2>/\Delta t$ plots, however, indicates that the best-fit line does not intercept the axis at the origin but at a value of $<\Delta d^2> \approx 0.2$ μm². This result suggests that a fast component might also be present in *Drosophila* embryos and yeast. In early nuclei, we did not find evidence of constraint for the long-range component for Δt up to 12 min. For longer time intervals, however, the motion of individual chromosomal loci appeared to be constrained to within a domain of approximately 3 μm radius. This radius of confinement is comparable to the dimensions of individual chromosomal territories, which maintained a relatively constant size throughout middle to late G2; these findings suggest that the domain explored by an individual locus represents a substantial portion of the volume occupied by the corresponding bivalent. Our data suggest that in early G2, loci diffuse at a relatively uniform rate within their chromosomal territory. In early spermatocytes, the three *lac* O sites tested appeared to be able to explore their respective domains within 30–60 min. The confinement of motion of individual loci to a small fraction of the nuclear volume suggests the tethering of the chromatin fiber to a limited number of sites within the nucleus. Such tethering would be consistent with the relatively fixed position of individual chromosomes observed in spermatocyte nuclei in middle G2 while allowing for substantial motion of individual loci within their territory.

Regulation of chromatin motion during the cell cycle

A comparison of the motion of well-defined loci at two different stages of the cell cycle revealed major differences in the rates and patterns of chromosome motion in early and late G2. The most striking difference was the absence of long-range motion in late G2 nuclei ($D < 1 \times 10^{-4}$ μm²/s). This absence of motion was difficult to establish when nuclei were imaged for relatively short intervals

(≤20 min) due to the lasting contribution of the short-range component and the effects of random deformations of the large, mature spermatocyte nuclei on interlocus distances. Statistical analysis of the data, however, clearly shows that the distribution of $<\Delta d>$ values does not significantly increase for time intervals greater than 1 min and indicates that most of the motion occurs in a short time scale. The absence of long-range motion was clearly demonstrated in nuclei imaged for extended periods of time. In late G2, individual loci appeared to occupy fixed positions within the nucleus for periods up to 10 hr. This was in contrast with the constant and rapid spatial reorganization of chromosomes in early G2.

Changes in the short-range motion of individual loci were also observed. The apparent short-range diffusion coefficient in early nuclei was about four times higher than that in late nuclei (1.3×10^{-2} versus 3.4×10^{-3} $\mu m^2/s$, respectively). These values correspond to average 3D step sizes of approximately 0.30 and 0.15 μm for individual loci in early and late nuclei, respectively. In early nuclei, we saw no significant differences in the motion of sister loci within individual nuclei. On the other hand, there was a great deal of variability in the motion patterns of sister loci in late nuclei. While these differences are difficult to quantitate, the analysis of time-lapse movies was consistent with late-nuclei motion patterns ranging from apparently immobile loci to loci subject to local Brownian motion comparable, within a factor of two, to that observed in early nuclei.

The different rates of chromatin motion in early and late nuclei, and the different rates of motion of sister loci within single nuclei in late G2, clearly suggest that chromosome motion can be regulated in the interphase nucleus. An explanation of these different rates would require major changes in the folding of the interphase chromatin fiber if the motion were the result of free diffusion. No global changes in chromosome size, shape, or compaction between early and late G2 nuclei were detected by DNA staining and light microscopy. Therefore we speculate that these differences in motion are primarily determined by interactions, specific and/or nonspecific, between chromatin and other nuclear components. Regulating such interactions would provide an efficient mechanism for regulating chromatin movements.

Regulatory implications

The different regimes of chromatin motion have implications for the regulation of genetic processes. Our results indicate a high level of local motion, with diffusion coefficients $\geq 1.3 \times 10^{-2}$ $\mu m^2/s$, within an approximately 0.3–0.7 μm range. As a comparison, the diffusion coefficient of much smaller biological macromolecules, such as mRNA, is only approximately 50 times higher [36]. These values are sufficient to allow for efficient local interactions, such as those required for enhancer-promoter association. Our results suggest that two sequences located less than approximately 1 μm apart have a very high probability of finding (interacting with) each other in a few seconds. We also found that individual chromosomal sites can explore a substantial fraction of their chromosomal territory within a few minutes. This motion could allow for relatively rapid remodeling of chromosome organization inside the nucleus and facilitate processes such as homology search and homologous chromosome pairing within the same chromosomal territory. On the other hand, chromosomes in early spermatocyte nuclei were confined to distinct territories for extended periods of time. Such a confinement is expected to result in a very small probability of interaction between sequences located on different chromosomes (excluding homologs), even in the presence of high chromosomal motility within a territory. Genetic studies have shown that the probability of interaction between chromosomal regions is strongly dependent on the relative position of those regions [37–39]. Our results are entirely consistent with these observations. On the other hand, in late G2, we found little or no long-range motion, and individual loci appeared to maintain relatively fixed positions within the nucleus for periods up to 10 hr, in agreement with the long-term preservation of nuclear organization observed in a variety of systems.

Conclusions

Our results have important implications for understanding interphase chromosome organization. We found evidence for complex patterns of motion of interphase chromosomes in live *Drosophila* spermatocytes. Our findings are consistent with different levels of organization of the chromatin fiber within the nucleus. The motion patterns in early G2 are characterized by a high degree of long-range motion and are consistent with the rapid remodeling of 3D chromosome structure. In late G2, on the other hand, there was little or no long-range motion, and this resulted in the preservation of chromosome organization for extended periods of time. The modulation of the long-range diffusion of chromatin over a ≥36-fold range during the cell cycle suggests that chromosome motility is not primarily determined by factors such as nuclear viscosity or chromosome crowding. Instead, we propose that the diffusive motion of chromosomes is under regulatory control within the parameters allowed by the physical constraints. Our results are most consistent with a mechanism involving interactions between the chromosomes and either the nuclear envelope [21] or other, molecularly undefined internal nuclear structures (Figure 7). The modulation of the number or the stability of these interactions could provide an economical means for regulating the range and rate of motion of chromatin. Our studies were conducted on a highly specialized cell-type, the premeiotic spermatocyte. It remains to be determined whether the patterns

Figure 7

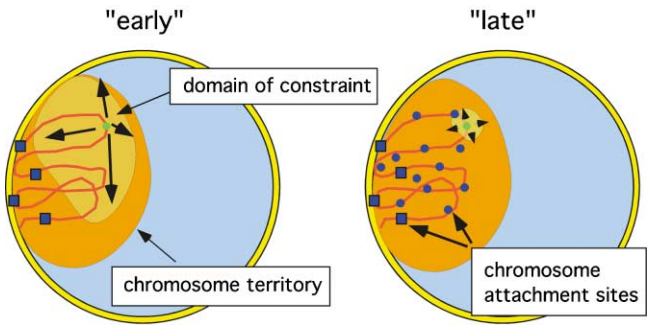

A model for chromosome organization and motion in spermatocyte nuclei. Spermatocyte nuclei in early and late G2 are shown schematically. Each chromosome territory contains a pair of replicated homologous chromosomes. In early nuclei, a few attachment sites define large chromosomal domains. This allows for a high degree of motion for individual loci while maintaining a fixed position for individual chromosomes within the nucleus. In late G2, a greater density of attachment sites constrains the motion of individual loci to a much smaller region. We propose that changes in the number of attachment sites and/or the stability of the interactions can modulate the rate and the range of chromatin motion.

of motion described here are specific to this particular cell type or if they are more general.

Materials and methods

Fly strains

The GFP-Lac repressor fusion protein (GFP-LacI) has been described [25, 28]. A truncated version of the bacterial Lac repressor protein lacking sequences necessary for tetramer formation was used for the prevention of adventitious interactions between individual *lac* O arrays. The fusion also contains a C-terminal SV40 NLS for nuclear targeting. An 880 bp DNA fragment from the 5′ regulatory region of the *Drosophila hsp83* gene was used for the expression of the GFP-LacI in the male germline [40]. The fusion protein was also cloned in vector pUASp [41]. This vector contains a P transposase promoter active in the *Drosophila* germline and a set of yeast GAL4 upstream activator sequences. pUASp can be used for ectopic expression of the fusion protein at high levels in a variety of tissues via the GAL4/UAS system [42]. Here, the vector was used as an enhancer trap [43] for recovering additional lines expressing the GFP-LacI in the male and female germline. Lines containing up to 256 copies of the *lac* operator direct repeat were generated by P element transformation, with the operator repeat cloned into the Casper 4 vector (A.S.B. et al, unpublished data). Germ line transformation was performed as described [44]. Additional lines carrying the *lac* O array were generated by mobilization of P element inserts. Chromosomal insertion sites of the *lac* O array were determined by in situ hybridization on polytene chromosomes.

In vitro tissue culture

Spermatocyte cysts were cultured in a sealed microscope chamber as described [30, 45], with minor modifications. Crawling third-instar male larvae were washed in distilled water, surface sterilized in 3% sodium hypochlorite, rinsed several times, and dissected in *Drosophila* SL3 tissue culture medium (GIBCO-BRL) supplemented with 7% fetal calf serum (S+). Two to four testes were transferred to a drop of S+ medium on a coverslip. For culture periods longer than 6 hr, the culture medium was supplemented with antibiotics (100 units/ml penicillin; 100 μg/ml streptomycin). The testis envelope was disrupted with a fine tungsten needle, allowing the release of individual cysts. The coverslip was mounted underneath a glass slide bearing a 0.5 inch hole, and the microscope chamber was completed with a second coverslip. The chamber was sealed with halocarbon oil. Under these conditions, the culture medium formed a column of approximately 2–3 mm diameter between the two coverslips. For adult testes, the anterior tip (approximately one third of total length) was severed, and a similar procedure was used. Morphological criteria were used for the identification of the developmental stages [29, 31].

2D and 3D Fluorescence Microscopy

2D and 3D time lapse images were acquired with a scientific-grade cooled CCD camera (Photometrics, Tucson, Arizona, USA) mounted on an Olympus IMT-2 inverted fluorescence microscope. Shutter action, stage movement, and data collection were automated with the IVE software platform [46]. A 60× 1.4 NA objective lens and immersion oil of N = 1.5180 (Cargille Laboratories, Cedar Grove, New Jersey, USA) were used. The pixel size was 0.11 × 0.11 μm in the x,y plane. The slight undersampling was offset by a corresponding sensitivity gain and represented an optimal compromise for the imaging of faint, moving fluorescent targets. To image GFP, we used the "Endow GFP" filter cube set (#41017; Chroma Technologies, Brattleboro, Vermont, USA). Typically, nuclei were imaged for 0.5 s. The actual times between consecutive images varied from about 1 to 2 s, depending on the size of the images collected (typically 256 × 256 or 512 × 512 pixels). For 3D data sets, z sections were collected at 0.25–0.4 μm intervals. Out-of-focus information was removed by a constrained iterative deconvolution method [47]. After manual selection of the appropriate nuclei, the identification of GFP dots and the distance measurements were performed automatically [46].

Under our imaging conditions, the cultured tissues remained healthy for up to 10–12 hr, as indicated by the absence of visible morphological changes and by the fact that spermatocytes, after up to 10 hr of culture, were able to successfully complete both meiotic divisions. Generally, spermatocytes could tolerate up to 600 0.5 s exposures over a 15 min period, and proportionally more if the exposures were spread over longer time periods. Morphological changes and developmental arrest were observed after longer periods in culture or after more intense imaging regimes.

Fluorescent latex beads (0.1 μm diameter MicroSpheres, Molecular Probes) were suspended in glycerol at approximately 2×10^8 particles/ml and were imaged under conditions similar to those used for live spermatocytes. Such beads showed diffusion coefficients comparable to that of chromatin and provided a control for unbiased and unconstrained random walks.

Data analysis

The data sets were tabulated as a time series (distance between pairs of GFP dots as a function of time). The mean square change in distance $<\Delta d^2>$ for individual data sets was computed and plotted with Minitab (Release 10 Xtra; Minitab Inc., State College, Pennsylvania) on an Apple G3 computer by the use of macros written in our laboratory. The same software package was used for the statistical analysis of the data and the correlation analysis. The position of individual dots was defined as the intensity-weighted center of mass. To empirically determine the error on the distance between dots, we took multiple measurements of the distance between standard fluorescent beads immobilized on a glass slide and found it to be approximately 0.04 μm, a value similar to that previously reported [21]. To obtain an estimate of the error on the distance measurements in a three-dimensional sample, we determined the distance between GFP dots in fixed spermatocyte nuclei (see Figure 3). The experimental error on these distances was approximately 0.07 μm. In early nuclei, we saw little or no large-scale nuclear deformations that would be likely to affect our estimate of the diffusion rates, and the MSD was independent of distance. Late nuclei were subject to random deformations of sufficient magnitude to affect our distance measurements. These effects were clearly identifiable in accelerated time lapse movies, and data sets in which these deformations were minimal were

used for diffusion measurements. These deformations occurred at random and lasted less than 10–20 s, which is relatively small compared to the average length of our data sets (≥10 min). Therefore, they had little impact on calculated diffusion coefficients, which represented averages over a large number of time points.

If d(t) is the measured 2D distance between two GFP dots at time t, the change in distance Δd for a given lag Δt is given by $d(t) - d(t + \Delta t)$. The mean square change in distance $<\Delta d^2>$ for $t = \Delta t$ was calculated as the average of the Δd^2 values over all possible combinations of time points separated by Δt. $<\Delta d^2>$ is equal to 2 × MSD, where MSD is the mean square displacement of the individual dots along each axis [21]. The translational diffusion coefficient D of individual dots is given by $D = MSD / 2\Delta t$ [48]. Therefore, in our experiments, $<\Delta d^2> = 4D\Delta t$. The average step size Δr_{rms} for individual dots, along each axis, is equal to $<\Delta d> / \sqrt{2}$. For a perfect random walk, the plot of MSD (or $<\Delta d^2>$) as a function of time should be a straight line with a slope characteristic of the diffusion coefficient of the GFP dots. As Δt increases, statistical fluctuations result in increasing error in the estimated MSD. For data sets with a large number of time points, the MSD values are fairly accurate for Δt values up to approximately one quarter of the entire data set and provide a good approximation of the diffusion coefficient [32, 33]. To ascertain that features of chromatin diffusion were not due to artifacts of instrumentation or data analysis, we similarly analyzed random walks generated by freely diffusing latex beads. Such random walks were undistinguishable from computer-generated, unbiased random walks.

Supplementary material

Time lapse movies of the motion of nuclei analyzed in Figure 3, as well as additional statistical analysis and figures, are available with this article on the internet at http://images.cellpress.com/supmat.supmatin.htm.

Acknowledgements

We thank members of the Belmont laboratory who helped create the initial fly lines containing the *lac* operator repeats; P. Rørth for the pUASp vector; and members of the Jan laboratory for their generous supply of *Drosophila* food and for access to their embryo microinjection facility. W. Marshall, J. Marko, M. Saxton, and H. Berg provided invaluable insights and suggestions about the mathematics of diffusion. We also thank R.S. Hawley, P. Schedl, U. Schibler, F. Jurnak, and D. Klionsky for their support and enthusiasm for this project as well as Jim Haber and members of the Sedat, Agard, and Cande labs for their critical comments and suggestions. This work was supported by NIH grants GM58460 and GM025101 to A.S.B. and J.W.S, respectively. J.V. was supported in part by a postdoctoral fellowship of the American Cancer Society-California Division (fellowship # 1-17-00).

References

1. Cremer T, Kurz A, Zirbel R, Dietzel S, Rinke B, Schrok E, *et al.*: **Role of chromosome territories in the functional compartmentalization of the nucleus.** *Cold Spring Harb Symp Quant Biol* 1993, **53:**777-793.
2. Lamond AI, Earnshaw WC: **Structure and function in the nucleus.** *Science* 1998, **280:**547-552.
3. Ellison JR, Howard GC: **Non-random position of the A-T rich DNA sequences in early embryos of Drosophila virilis.** *Chromosoma* 1981, **83:**555-561.
4. Marshall WF, Dernburg AF, Harmon B, Agard DA, Sedat JW: **Specific interactions of chromatin with the nuclear envelope: positional determination within the nucleus in Drosophila melanogaster.** *Mol Biol Cell* 1996, **7:**825-842.
5. Dernburg AF, Broman KW, Fung JC, Marshall WF, Philips J, Agard DA, *et al.*: **Perturbation of nuclear architecture by long-distance chromosome interactions.** *Cell* 1996, **85:**745-759.
6. Csink AK, Henikoff S: **Genetic modification of heterochromatic association and nuclear organization in Drosophila.** *Nature* 1996, **381:**529-531.
7. Csink AK, Henikoff S: **Large-scale chromosomal movements during interphase progression in Drosophila.** *J Cell Biol* 1998, **143:**13-22.
8. Hiraoka Y, Dernburg AF, Parmelee SJ, Rykowski MC, Agard DA, Sedat JW: **The onset of homologous chromosome pairing during Drosophila melanogaster embryogenesis**. *J Cell Biol* 1993, **120:**591-600.
9. Fung JC, Marshall WF, Dernburg A, Agard DA, Sedat JW: **Homologous chromosome pairing in Drosophila melanogaster proceeds through multiple independent initiations.** *J Cell Biol* 1998, **141:**5-20.
10. Gerasimova TI, Byrd K, Corces VG: **A chromatin insulator determines the nuclear localization of DNA.** *Mol Cell* 2000, **6:**1025-1035.
11. Heun P, Laroche T, Rhaguraman MK, Gasser SM: **The positioning and dynamics of origins of replication in the budding yeast nucleus.** *J Cell Biol* 2001, **152:**385-400.
12. Dimitrova DS, Gilbert DM: **The spatial position and replication timing of chromosomal domains are both established in early G1 phase.** *Mol Cell* 1999, **4:**983-993.
13. Brown KE, Guest SS, Smale ST, Hahm K, Merkenschlager M, Fisher AG: **Association of transcriptionally silent genes with Ikaros complexes at centromeric heterochromatin.** *Cell* 1997, **91:**845-854.
14. Brown KE, Baxter J, Graf D, Merkenschlager M, Fisher AG: **Dynamic repositioning of genes in the nucleus of lymphocytes preparing for cell division.** *Mol Cell* 1999, **3:**207-217.
15. Schubeler D, Francastel C, Cimborra DM, Reik A, Martin DI, Groudine M: **Nuclear localization and histone acetylation: a pathway for chromatin opening and transcriptional activation of the human beta-globin locus.** *Genes Dev* 2000, **14:**940-950.
16. Francastel C, Schubeler D, Martin DI, Groudine M: **Nuclear compartmentalization and gene activity.** *Nat Rev Mol Cell Biol* 2000, **1:**137-143.
17. Lundgren M, Chow CM, Sabbattini P, Georgiou A, Minnaee S, Dillon, N: **Transcription factor dosage affects changes in higher order chromatin structure associated with activation of a heterochromatic gene.** *Cell* 2000, **103:**733-743.
18. Tumbar T, Belmont AS: **Interphase movements of a DNA chromomsome region modulated by VP16 transcriptional activator.** *Nat Cell Biol* 2001, **3:**134-139.
19. Gasser SM: **Positions of potential: nuclear organization and gene expression.** *Cell* 2001, **104:**639-642.
20. Mahy NL, Bickmore WA, Tumbar T, Belmont AS: **Linking large-scale chromatin structure with nuclear function.** In *Chromatin Structure and Gene Expression***.** Edited by Elgin SCR and Workman JL. Oxford, UK: Oxford University Press. 2000.
21. Marshall WF, Straight A, Marko JF, Swedlow J, Dernburg A, Belmont A, *et al.*: **Interphase chromosomes undergo constrained diffusional motion in living cells.** *Curr Biol* 1997, **7:**930-939.
22. Cremer T, Cremer C, Baumann H, Luedtke EK, Sperling K, Teuber V, *et al.*: **Rabl's model of the interphase chromosome arrangement tested in Chinese hamster cells by premature chromosome condensation and laser-UV-microbeam experiments.** *Hum Genet* 1982, **60:**46-56.
23. Abney JR, Cutler B, Fillbach ML, Axelrod D, Scalettar BA: **Chromatin dynamics in interphase nuclei and its implications for nuclear structure.** *J Cell Biol* 1997, **137:**1459-1468.
24. Zink D, Cremer T, Saffrich R, Fischer R, Trendelenburg MF, Ansorge W, *et al.*: **Structure and dynamics of human interphase chromosome territories in vivo.** *Hum Genet* 1998, **102:**241-251.
25. Straight AF, Belmont AS, Robinett CC, Murray AW: **GFP tagging of budding yeast chromosomes reveals that protein-protein interactions can mediate sister chromatid cohesion.** *Curr Biol* 1996, **6:**1599-1608.
26. Gordon GS, Sitnikov D, Webb CD, Teleman A, Straight A, Losick R, *et al.*: **Chromosome and low copy plasmid segregation in *E. coli*: visual evidence for distinct mechanisms.** *Cell* 1997, **90:**1113-1121.
27. Teleman AA, Graumann PL, Lin DC, Grossman AD, Losick R: **Chromosome arrangement within a bacterium.** *Curr Biol* 1998, **8:**1102-1109.
28. Robinett CC, Straight AF, Li G, Willhelm C, Sudlow G, Murray A, *et al.*: **In vivo localization of DNA sequences and visualization of large-scale chromatin organization using *lac* operator/repressor recognition.** *J Cell Biol* 1996, **135:**1685-1700.
29. Fuller MT: **Spermatogenesis.** In *The Development of Drosophila*. Edited by M. Bate and A. Martinez-Arias. Cold Spring Harbor, New York: Cold Spring Harbor Press; 1993:71-147.
30. Cross DP, Shellenbarger DL: **The dynamics of Drosophila melanogaster spermatogenesis in in vitro cultures.** *J Embryol Exp Morphol* 1979, **53:**345-351.
31. Cenci G, Bonaccorsi S, Pisano C, Verni F, Gatti M: **Chromatin and microtubule organization during premeiotic, meiotic and early postmeiotic stages of Drosophila melanogaster spermatogenesis.** *J Cell Sci* 1994, **107:**3521-3534.

32. Qian H, Sheetz MP, Elson EL: **Single particle tracking. Analysis of diffusion and flow in two- dimensional systems.** *Biophys J* 1991, **60:**910-921.
33. Saxton MJ: **Single-particle tracking: the distribution of diffusion coefficients.** *Biophys J* 1997, **72:**1744-1753.
34. Saxton MJ: **Anomalous diffusion due to obstacles: a Monte Carlo study.** *Biophys J* 1994, **66:**394-401.
35. Diggle PJ: *Time Series. A Biostatistical Introduction*. New York: Oxford Science Publications, Oxford University Press; 1990.
36. Politz JC, Tuft RA, Pederson T, Singer RH: **Movement of nuclear poly(A) RNA throughout the interchromatin space in living cells.** *Curr Biol* 1999, **9:**285-291.
37. Hilliker AJ: **Assaying chromosome arrangement in embryonic interphase nuclei of Drosophila melanogaster by radiation induced interchanges.** *Genet Res* 1985, **47:**13-18.
38. Sachs RK, Chen AM, Brenner DJ: **Review: proximity effects in the production of chromosome aberrations by ionizing radiation.** *Int J Radiat Biol* 1997, **71:**1-19.
39. Burgess SM, Kleckner N: **Collisions between yeast chromosomal loci in vivo are governed by three layers of organization.** *Genes Dev* 1999, **13:**1871-1883.
40. Yue L, Karr TL, Nathan DF, Swift H, Srinivasan S, Lindquist SL: **Genetic analysis of viable Hsp90 alleles reveals a critical role in Drosophila spermatogenesis.** *Genetics* 1999, **151:**1065-1079.
41. Rorth P: **Gal4 in the Drosophila female germline.** *Mech Dev* 1998, **78:**113-118.
42. Brand AH, Perrimon N: **Targeted gene expression as a means of altering cell fates and generating dominant phenotypes.** *Development* 1993, **118:**401-415.
43. Wilson C, Pearson RK, Bellen HJ, O'Kane CJ, Grossniklaus U, Gehring WJ: **P-element-mediated enhancer detection: an efficient method for isolating and characterizing developmentally regulated genes in Drosophila.** *Genes Dev* 1989, **3:**1301-1313.
44. Rubin GM, Spradling AC: **Genetic transformation of Drosophila with transposable element vectors.** *Science* 1982, **218:**348-353.
45. Forer A: **Crane fly spermatocytes and spermatids: a system for studying cytoskeletal components.** *Meth Cell Biol* 1982, **25 Pt B:** 227-252.
46. Chen H, Hughes DD, Chan TA, Sedat JW, Agard DA: **IVE (image visualization environment): a software platform for all three-dimensional microscopy applications.** *J Struct Biol* 1996, **116:**56-60.
47. Agard DA, Hiraoka Y, Shaw P, Sedat JW: **Fluorescence microscopy in three dimensions.** *Meth Cell Biol* 1989, **30:**353-377.
48. Berg HC: *Random Walks in Biology*. Princeton, New Jersey: Princeton University Press; 1993.